

Faster Data Collection Without Loss of Precision. An Extension of the Learnt Profile Method

BY WILLIAM CLEGG

*Anorganisch-Chemisches Institut der Universität, Tammannstrasse 4, D-3400 Göttingen,
Federal Republic of Germany*

(Received 18 April 1980; accepted 2 June 1980)

Abstract

The method of fitting a learnt and continually revised profile to X-ray diffraction step-scan measurements, previously described for protein crystals and a linear diffractometer, has been modified and extended for a wider range of samples and a four-circle diffractometer. Variation of peak width is dealt with by assuming an anisotropic functional form, the parameters for which are derived by least-squares refinement from measurements of selected strong reflexions. The effect of the α doublet on the reflexion shape is treated by an empirical method, which extracts α_1 and α_2 components from the observed profile with a minimum of assumptions. Several internal consistency tests are made to test the validity of the method for every measured reflexion, and possible errors are flagged. Application of the method enables a considerable increase in data-collection speed over conventional methods, without corresponding loss of precision. Typical rates of data collection by this method are 100 reflexions per hour, or 2–3 medium-sized structures per week, for a Stoe–Siemens AED diffractometer and a 2 kW tube (Mo $K\alpha$ radiation, graphite monochromator).

1. Introduction

The quantities of interest in single-crystal data collection by X-ray diffraction are the integrated intensity I and its e.s.d. $\sigma(I)$ for each reflexion. Different methods have been described for obtaining these quantities from measured reflexion profiles. The simplest of all is the background-peak-background (BPB) method, in which the integration is performed at the time of measurement and the individual points of the profile are ignored. In this method, the background measurements may be stationary, or may themselves be the sum of the outer points of the profile measurement. Various improvements to this basic method have been proposed, usually with one or more of the aims: (i) to allow for misplaced reflexion peaks, caused by crystal

movement and/or inaccurate unit cell and orientation parameters; (ii) to reduce the width of the scan required; (iii) to reduce counting times (and hence, in many cases, crystal decomposition in the X-ray beam) without loss of precision; (iv) to improve precision for a given measurement time. These improvements make use of the individual profile points rather than their sum alone.

The ordinate analysis method (Watson, Shotton, Cox & Muirhead, 1970) locates the centre of a reflexion by finding the n adjacent profile points giving maximum net intensity. This method has been criticized for introducing systematic bias in the weak reflexions by Tickle (1975), who suggests instead that the peak centre be determined as the median of the measured profile. The peak intensity is then the sum of the n points centred on the median and the remaining points constitute the background.

More complex methods, in which the dividing points between the peak and each background are determined by analysing each reflexion profile, include those of Bartl & Schuckmann (1966) and Slaughter (1969). The $\sigma\mathcal{S}/\mathcal{S}$ method of Lehmann & Larsen (1974) was developed for neutron diffraction studies and is not applicable to X-rays without some empirical modification (Blessing, Coppens & Becker, 1974). A selection of profile-analysis methods has been examined in detail by van der Wal, de Boer & Vos (1979). The object of each of these methods is to determine the optimum division of the measured profile into reflexion peak and background regions. Once this is achieved, the net intensity is obtained by subtracting the total background count from the total peak count (after suitable scaling if the numbers of points are unequal in the two regions). The optimizing process, whichever it is, increases the value of $I/\sigma(I)$ compared with the traditional BPB method.

A fundamentally different approach is to fit the sum of a peak function and a background function to the observed profile, and thus to derive least-squares estimates of I and $\sigma(I)$. Norrestam (1972) and Hanson, Watenpaugh, Sieker & Jensen (1979) have used a

Gaussian peak function, fitted to a much smaller number of points than is usual for any of the BPB-based methods described above. The use of a standard peak function effectively combats the adverse effect on the $I/\sigma(I)$ ratio of the reduced total time spent on reflexion measurement. The assumption of a Gaussian shape for the reflexion profile is reasonable, provided that measurements are not made at sufficiently high angles to produce significant α_1 - α_2 splitting. This is usually the case in protein crystallography with Cu $K\alpha$ radiation. The problem is greater for Mo $K\alpha$ radiation, commonly used for inorganic and organometallic studies, because the doublet resolution is relatively greater (Norrestam, 1972).

In the method of Diamond (1969), a stored normalized profile is used for fitting, instead of an analytical function. The stored profile is learnt from the particular crystal under investigation, and is continually revised during the data collection, each measured reflexion of significant intensity making a contribution to it. This method has the advantage of not assuming a particular functional form of the reflexion profile, and is particularly effective for weak reflexions. A limited degree of variation of reflexion shape is allowed for by the profile learning process. Here again, the α -doublet separation is a problem. In this paper we present a method of dealing both with this problem and also with variations in profile width produced by anisotropy of crystal mosaic spread and non-uniformity of crystal dimensions (e.g. for needle and plate crystals, for which the effects can be severe), thus making the method of Diamond much more generally applicable.

Familiarity with the basic points of Diamond's (1969) method is assumed as a foundation for the following sections.

2. Principle

We tackle the two problems separately. If we had a source of pure $K\alpha_1$ radiation without $K\alpha_2$, all reflexions would be of approximately the same form, but the width would vary because of various anisotropic factors, and would also increase with Bragg angle because of wavelength dispersion within the still not strictly monochromatic $K\alpha_1$ band. Superimposed on this width variation is the effect of the α doublet. At low Bragg angles, the $K\alpha_1$ and $K\alpha_2$ reflexions are virtually superimposed, but with increasing θ , the $K\alpha_2$ reflexion gradually emerges on the high- θ side, introducing asymmetry into the combined reflexion form because of its lower intensity. If the reflexions are narrow enough, the two peaks may be resolved at high angles.

The basic principle of our method is to extract from the measured profile of each reflexion the α_1 and α_2 components, regardless of Bragg angle, and with as few assumptions as possible about their form. The two

separated components are then superimposed and summed, to produce a pure-component peak. Variations in the width of this peak over reciprocal space are fitted by a simple function, which is derived for each crystal before data collection begins, and from which the correct scan parameters are calculated for each reflexion. The learnt profile corresponds to a pure-component peak, *i.e.* has the effects of α -doublet separation removed from it, and the profile-learning process which takes place during data collection effectively makes fine-tuning adjustments to the initially determined width parameters. Like Diamond, we always fold reflexion profiles about their medians before fitting the learnt profile to them; in our case, this folding is performed on the pure-component peak, *i.e.* after separation and superposition of the α_1 and α_2 components. The learnt profile is then a set of $n/2$ points for an n -point scan.

According to Diamond, the optimum scan width for the profile method is about twice the peak width (base to base) or a little less, but for a linear diffractometer, mis-centring of the reflexions in the scan sets a lower limit on the possible scan width which may be greater than this optimum value. For a four-circle diffractometer, stable crystal, and accurate crystal orientation matrix, mis-centring is less of a problem. We set the desired scan width in ω at about 1.5 times the expected width of the pure-component peak, plus the α_1 - α_2 separation. This expected width is taken as $8s$, where s is the r.m.s. width of the folded profile for the reflexion peak (Diamond's σ). Thus the scan width is $W = 12s$ for the pure-component peak. In practice, we have to make a wider scan, because our diffractometer circles can only be set to 0.01° , and the scan interval must be rounded up to the next multiple of 0.01° .

To determine the expected pure-component peak width and hence the scan parameters for a reflexion, we assume that W can be described for all reflexions by a seven-parameter function, of the same form as that used by Hanson *et al.* (1979):

$$W = \sum \sum a_i a_j A_{ij} + B \tan \theta \quad (1)$$

where the a_i are the direction cosines of the diffraction vector relative to a crystal-fixed set of Cartesian axes, and A is a symmetric 3×3 tensor. The term $B \tan \theta$ allows for wavelength dispersion *within* α_1 and α_2 , but not for the α_1 - α_2 separation itself, which is treated separately, as described in the next section. The values of B and the components of A are determined for each crystal before data collection begins.

3. Method

Let us assume that we already have values for the scan-width parameters A_{ij} and B and an initial folded

profile P of $n/2$ points. The following steps are required for each reflexion to be measured.

(i) From the indices and orientation matrix, calculate *inter alia* W from (1). Calculate $\Delta\omega' = W/(n - 1)$, then round it up to the next multiple of 0.01° to give the scan interval $\Delta\omega$. The ratio f of scan intervals for crystal (ω) and counter (2θ) is specified by the user, $\Delta 2\theta = f\Delta\omega$. We generally set $f = 1$ (a θ/ω scan), which is a compromise between the relative advantages and disadvantages of the ω scan ($f = 0$) and the $2\theta/\omega$ scan ($f = 2$) [see, for example, Werner (1972) and Alexander & Smith (1964)].

(ii) To allow for the α_1 - α_2 separation, increase the number of points in the scan, $m = n + \lfloor \theta(\alpha_1 - \theta(\alpha_2))/\Delta\omega \rfloor$, rounded up to the next integer.

(iii) Scan the reflexion for m points, beginning at an angle $(n - 1)\Delta\omega/2$ below the expected α_1 position, with a minimum counting time per step, as specified by the user. This gives an array V of m points.

(iv) Calculate the position of the median and from it initial values for the α_1 and α_2 peak positions [from the known $\lambda(\alpha_1)$, $\lambda(\alpha_2)$ and $\lambda(\bar{\alpha})$ wavelengths].

(v) Set up two arrays X and Y , each of m points, corresponding to two peaks centred on these α_1 and α_2 positions. The value for each point is calculated from the current learnt profile, by interpolation, allowing for the expected mismatch $\Delta\omega/\Delta\omega'$ of widths, *i.e.* the arrays X and Y represent the expected ideal α_1 and α_2 reflexion profiles for the reflexion as measured. All interpolations performed in this method are by the four-point Lagrangian formula

$$\begin{aligned} X_{n+p} = & -\frac{1}{6}p(p-1)(p-2)X_{n-1} \\ & + \frac{1}{2}(p+1)(p-1)(p-2)X_n \\ & - \frac{1}{2}(p+1)p(p-2)X_{n+1} \\ & - \frac{1}{6}(p+1)p(p-1)X_{n+2} \end{aligned}$$

where n is an integer and $0 \leq p < 1$.

(vi) Take an average of the few extreme low-angle points of V and another of the extreme high-angle points. Use these to calculate a crude linear sloping background for the reflexion in array Z and subtract the points of Z from V . This step facilitates the following empirical separation of the α_1 and α_2 peaks. If the measured reflexion has a median so far off-centre that no background is observed at one end of the scan, the reflexion is flagged as an error, and not further treated. This occurs rarely if the crystal is securely mounted.

(vii) Scale the arrays X and Y , so that $V_i = 1.5X_i = 3Y_i$, *i.e.* in the expected $\alpha_1:\alpha_2$ intensity ratio of 2:1 (for Mo $K\alpha$).

(viii) Adjust the individual points of X and Y , so that $X_i + Y_i = V_i$, by multiplying each by $1 + (V_i - X_i - Y_i)/(X_i + Y_i)$. The effect of this is to compare V_i with $X_i + Y_i$ and to distribute the excess (or deficit) in V_i between X_i and Y_i in the ratio of their initial values.

(ix) Divide each point of Z between X and Y , increasing X_i by $\frac{2}{3}Z_i$ and Y_i by $\frac{1}{3}Z_i$. Calculate the medians of X and Y .

The net effect of steps (iv) to (ix) is to extract from the observed reflexion profile the α_1 and α_2 components. In setting up initial components [steps (iv) to (vii)], the assumptions are made that both components have the same form, which is that of the current learnt profile, that they occur with the expected separation (though not necessarily at exactly the expected positions in the scan), and that they have an intensity ratio of 2:1. In step (viii), these constraints are effectively relaxed, so that the resulting components represent a balance between reasonable assumptions and observed measurements. We have tried a variety of methods for extracting the α_1 and α_2 components from the measured profile, most of them involving iterative calculations, but the method finally chosen and described here is the simplest, gives the best results, and imposes the fewest constraints. Its results are subjected to extensive internal checking, as described in the next steps, and its validity is borne out by its success (see §§ 6 and 7).

(x) Fold the two components about their medians and add the two results together. The n -point array obtained is a pure-component peak for this reflexion but, because of the rounding up of $\Delta\omega$, the width does not match that of the learnt profile.

(xi) Interpolate the observed profile array to adjust its width by the ratio $\Delta\omega/\Delta\omega'$. The folding and superposition of the component peaks has something of a smoothing effect, so this interpolation works well, even for weak reflexions.

(xii) Fit the sum of the learnt profile P and a flat background to this derived reflexion profile Q , to obtain least-squares values for the intensity I and its e.s.d. $\sigma(I)$, from equations (13), (15) and (16) of Diamond (1969).

(xiii) Calculate alternative values of I and $\sigma(I)$ by the BPB method. For this purpose, the original measured profile V is used, and the peak is considered to be composed of all points within $4s_p$ of either the α_1 or α_2 peak positions determined in step (iv); s_p is here the r.m.s. width of the current learnt profile. This calculation is completely independent of steps (v) to (xii), and so provides an internal check on the results obtained from the profile extraction and fitting.

(xiv) Select the result giving lower $\sigma(I)$, but if the residual $\sqrt{2R/n}$ for the profile fit is >1.3 , select the BPB result. If $I/\sigma(I)$ is greater than a pre-selected value, continue with step (xv). Otherwise, estimate the counting time per step required to achieve this desired precision. If it can be attained within a prescribed maximum time, remeasure the reflexion for the extra time required, combine the two measurements in V and return to step (iv). If the desired precision cannot be attained within the given maximum time, set a default measuring time chosen by the user. If this is greater

than the minimum time, remeasure for the extra time and return to step (iv).

(xv) Calculate the r.m.s. width of the profile Q for diagnostic purposes (s_Q).

(xvi) Update the learnt profile. The contribution of Q to the profile (after subtraction of background and normalization) is

$$q = \frac{(I/I_0)^2}{1 + (I/I_0)^2} \quad (2)$$

such that P is replaced by $(1 - q)P + qQ$. The constant I_0 is usually taken as half the maximum intensity so far found for any reflexion, though it can be altered to give either more- or less-rapid updating of the profile, and the contribution q is reduced for reflexions giving a poor profile fit.

(xvii) Output results. For each reflexion the output contains *inter alia* indices, I , $\sigma(I)$, $\Delta\omega$, measuring time, q , and a set of diagnostic flags and values. These values include the profile-fit residual, the difference (expressed in e.s.d.'s) between the profile and BPB results, the discrepancy between learnt and observed profile widths (s_p and s_Q), and the discrepancy between expected and observed peak median positions. Reflexions are flagged for diagnostic purposes when discrepancy values exceed preset limits. At intervals during data collection, when standard reflexions are measured, running totals of all flags are printed out.

4. Obtaining initial parameters

Before data collection begins, we must obtain values for the scan-width parameters (A_{ij} and B) and an initial profile. We use the data-collection routine itself for this purpose, with a few modifications.

The first step is to assume an isotropic width function,

$$W = A + B \tan \theta \quad (3)$$

instead of the anisotropic form given in (1), and to set up an initial profile of Gaussian form, with $s_p = (n - 1)/12$ (expressed here in number of steps rather than degrees). Rough values of A and B are obtained by estimating the widths at half-height of one low- θ and one high- θ reflexion. These two reflexions are entered into a list, together with a number (between about 20 and 50) of others, which are chosen to cover reciprocal space as widely as possible (such reflexions of medium to high intensity are generally already available from the preliminary investigations of unit cell, orientation, space group, etc.).

A preliminary data collection is now performed for these reflexions, with the method already described, but with the following modifications:

(a) After the first two reflexions have been measured, the derived r.m.s. widths s_Q [step (xv)] are

used to obtain improved estimates of A and B in (3) for W .

(b) The value of s_Q for each reflexion is stored.

(c) The profiles V , X and Y are printed.

(d) After step (xv), the profile Q is further interpolated to produce a peak with $s_Q = W/12$ (in degrees) = $(n - 1)/12$ (in steps). When the learnt profile is updated, this extra interpolation maintains an almost constant s_p , compensating for deviations from the isotropic approximation for W . The effect is to produce an initial learnt profile which corresponds to the form of the reflexions for the particular crystal being studied, allowing for width variations.

(e) In the profile updating step, the contribution for the j th reflexion is

$$q = 1/(j + 1)$$

instead of the expression in (2). This produces an equal contribution from each reflexion to the initial profile.

(f) The values of I and $\sigma(I)$ are ignored.

After all reflexions in the list have been measured, the parameters A_{ij} and B are determined by a least-squares fit of the s_Q values, and data collection proper can begin. Output from this initializing routine contains the derived A_{ij} and B parameters with e.s.d.'s, the starting profile, and a list of observed and calculated reflexion widths with their differences. Reflexions with unusual shapes can be recognized from the printed widths and the full V , X and Y arrays, investigated, and removed from the list if necessary. The routine can be executed again, in which case the already derived profile and width parameters are available as initial estimates. The time required for our equipment is normally less than 1 min per reflexion.

5. Implementation

The method is in use for a Stoe-Siemens AED four-circle diffractometer with graphite-mono-chromated Mo $K\alpha$ radiation. This instrument combines high mechanical precision with fast positioning of the circles. The motors, shutters, counting-chain and associated devices are controlled by a microprocessor, which receives instructions from and returns results to a host computer. The microprocessor, its ROM resident program, and suitable assembly routines for the interface with the host computer were supplied with the diffractometer. The control program, which replaces that supplied, is written in Basic for a Data General Eclipse S250 mini-computer, and runs in time-shared mode with other Basic programs and with Fortran programs for structure solution, refinement, plotting, etc. The advantages of Basic include (i) the suitability of the supplied assembler subroutines without major modification; (ii) the time-sharing configuration of Data

General's Multiuser Basic system; (iii) the ease of program modification. The major disadvantage is the slow execution speed compared with, for example, Fortran. Thus, the process of extracting and fitting a profile takes several seconds. In order not to waste this time, before beginning the process, we send an instruction to the microprocessor to reset the circles to the beginning of the scan (we scan always in the same direction to avoid the effects of backlash and/or uncertainty in the circle position sensors, which amount to about 0.01°), or for the next reflexion if the current reflexion has already been scanned twice. This is a form of internal time-sharing, and saves about 5% of total data-collection time on average, at the cost of further complication of the program.

Further comments which are relevant to the data-collection method are:

(i) Tests have indicated that the profile-fitting method produces considerable improvement in the $I/\sigma(I)$ ratio for a given measuring time, the value of $\sigma(I)$ being decreased by a factor >2 in many cases for weak reflexions. Alternatively stated, for such reflexions we can attain the same precision with *less than a quarter* of the counting time required by the traditional BPB method.

(ii) Our data-collection strategy of scanning all reflexions for a minimum time, then for an additional time if required, is approximately a constant-precision rather than a constant-time method. Such methods have been described previously (*e.g.* Grant, 1973; Freeman, Guss, Nockolds, Page & Webster, 1970) and are preferable because of the more effective use of data-collection time and the greater suitability of the data for least-squares refinement. Typical settings are: number of steps $n = 24$, desired $I/\sigma(I) = 20$, minimum time per step = 0.5s, maximum time = 2 or 3s, default time = minimum time. Thus the weakest reflexions are measured only at the fastest speed, but *no* reflexions (other than those with a calculated median grossly in error, or systematic absences due to lattice centring) are skipped. The inclusion of the weakest reflexions in the data set is important for structure solution by certain direct methods (*e.g.* when negative quartets are to be used); such reflexions, with $I < k\sigma(I)$ (k in the range 1–3) are commonly discarded for structure refinement.

(iii) Special measurement procedures are incorporated within the same data-collection routine, as options selected by user-set flags. Special procedures currently incorporated are (a) measurement of reflexions at a series of azimuthal angle settings, for empirical absorption correction calculations (the azimuthal angle ψ is included in the output) and (b) measurement of Friedel pairs on opposite sides of the incident beam so that the absorption correction is approximately the same for both reflexions if the crystal shape is symmetrical for absolute configuration studies.

6. Examples of profile extraction

The figures show examples of the α_1 - α_2 profile extraction. The crystal for Fig. 1 was an antimony oxide derivative and was extensively used for testing purposes because of its extreme crystal shape [a thin needle giving anisotropic width parameters $A_{11} = 0.63$ (3), $A_{22} = 0.92$ (4), $A_{33} = 0.83$ (2), $A_{23} = 0.01$ (2), $A_{13} = 0.01$ (3), $A_{12} = 0.00$ (3), $B = 0.02$ (6), derived from 28 reflexions], its intense scattering even at high angles, and the narrowness of the reflexions. Results are shown for four reflexions of different Bragg angles. These strong reflexions (relative intensities *ca* 10:10:2:1) give high profile-fit residuals, as expected (2.0, 1.6, 3.0 and 3.0 respectively), but for all four the values obtained for I by the profile and BPB methods

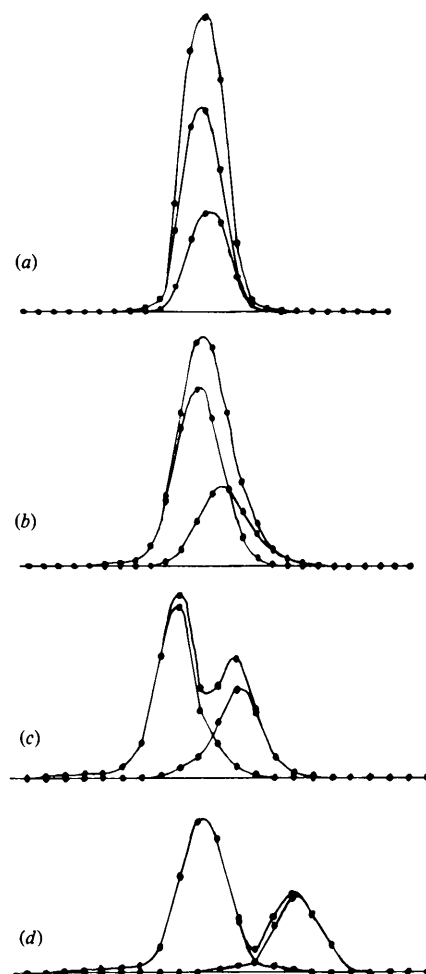


Fig. 1. Examples of profile extraction for a crystal with a high degree of α -doublet resolution. The reflexions are from different regions of reciprocal space: (a) $\theta = 4.93^\circ$, measured at 25 points, $\Delta\omega = 0.04^\circ$; (b) $\theta = 13.86^\circ$, 27 points, $\Delta\omega = 0.04^\circ$; (c) $\theta = 28.61^\circ$, 27 points, $\Delta\omega = 0.05^\circ$; (d) $\theta = 36.14^\circ$, 30 points, $\Delta\omega = 0.05^\circ$. The outer background points of the wider scans are omitted.

are insignificantly different (the largest discrepancy is $I_{\text{profile}} - I_{\text{BPB}} = -1.2[\sigma^2(I_{\text{profile}}) + \sigma^2(I_{\text{BPB}})]^{1/2}$ for reflexion (d)). This crystal is an extreme case, the α_1 - α_2 resolution being otherwise rarely complete.

A second crystal (a complex of copper with bridging ligands) (Fig. 2) is more typical, the reflexions being broader and the α doublet remaining incompletely resolved at the highest Bragg angles measured. The four reflexions shown have relative intensities *ca* 3:2.5:1:1 and are all $0k0$ reflexions, so the width variation is entirely accounted for by the α -doublet splitting and the wavelength dispersion [$B = 0.78$ (3)]. In this case, the A_{ij} components are $A_{11} = 0.524$ (6), $A_{22} = 0.518$ (6), $A_{33} = 0.525$ (6), $A_{23} = -0.003$ (3), $A_{13} = 0.002$ (5), $A_{12} = -0.005$ (7), derived from 20 reflexions. Profile-fit residuals for the four reflexions are 2.6, 1.6, 0.9 and 1.2, and for all four reflexions the discrepancy $|I_{\text{profile}} - I_{\text{BPB}}|$ is $< 0.8[\sigma^2(I_{\text{profile}}) + \sigma^2(I_{\text{BPB}})]^{1/2}$. This discrepancy shows no systematic trends with intensity or profile-fit residual.

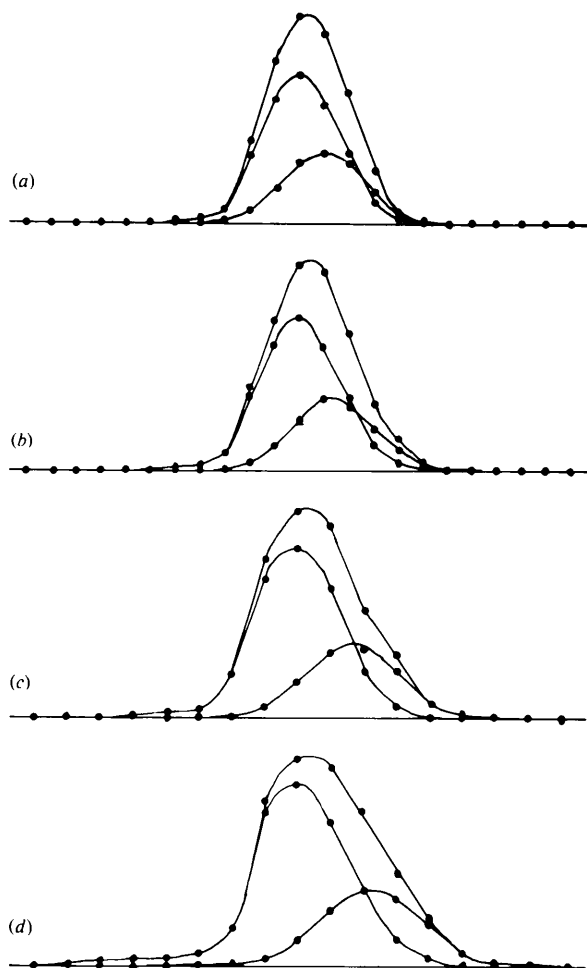


Fig. 2. Profiles of four reflexions from one reciprocal-lattice row: (a) $\theta = 5.60^\circ$, 26 points, $\Delta\omega = 0.03^\circ$; (b) $\theta = 8.41^\circ$, 26 points, $\Delta\omega = 0.03^\circ$; (c) $\theta = 14.11^\circ$, 27 points, $\Delta\omega = 0.04^\circ$; (d) $\theta = 17.01^\circ$, 27 points, $\Delta\omega = 0.04^\circ$.

7. Results

This method has been used to collect 58 sets of data in eight months. The subjects studied have been drawn from organic, organometallic and inorganic chemistry, with a wide variety of unit-cell sizes and symmetries, mosaic spreads, proportions of weak and strong reflexions and crystal qualities. Final *R* indices for crystals of medium to high quality are typically in the range 0.03–0.06; higher values can usually be traced to poor crystal quality, disorder, high thermal motion, or other factors dictated by the crystal rather than the data collection. With the typical data-collection parameters given in § 5, the average rate of data collection is 100 reflexions per hour. We have a rule of thumb that the total diffractometer time required for a crystal, including all preliminary investigations (cell and space-group determination, *etc.*) as well as data collection itself, is about 1.5 h per independent non-hydrogen atom. Thus, an average of three 50- to 60-atom structures can be investigated per week, assuming no time is lost by machine faults, program development, *etc.*

8. Summary

The method described here is a development of the established learnt-profile analysis of X-ray reflexions, and makes possible a considerable increase in the rate of data collection without loss of precision, when compared with methods which perform little or no analysis of the individual points of the reflexion profile. The method also has a high degree of internal consistency checking. Results obtained so far demonstrate its general applicability and validity. It is worth noting that with small modifications it could be used for off-line processing of profile data; the on-line application is convenient and useful in reducing the full profile to a final output of *I* and $\sigma(I)$, and is valuable in selecting the appropriate counting-time to give approximately constant-count statistics, but is not essential.

I thank my colleagues for their patience over several weeks in which the diffractometer was unavailable for data collection during program development and testing, Professor G. M. Sheldrick for suggestions and encouragement and Dr M. Noltemeyer for technical assistance.

References

- ALEXANDER, L. E. & SMITH, G. S. (1964). *Acta Cryst.* **17**, 1195–1201.
 BARTL, M. Z. & SCHUCKMANN, W. (1966). *Neues Jahrb. Mineral. Monatsh.* **4**, 126–130.
 BLESSING, R. H., COPPENS, P. & BECKER, P. (1974). *J. Appl. Cryst.* **7**, 488–492.

- DIAMOND, R. (1969). *Acta Cryst.* A25, 43–55.
 FREEMAN, H. C., GUSS, J. M., NOCKOLDS, C. E., PAGE, R. & WEBSTER, A. (1970). *Acta Cryst.* A26, 149–152.
 GRANT, D. F. (1973). *Acta Cryst.* A29, 217.
 HANSON, J. C., WATENPAUGH, K. D., SIEKER, L. & JENSEN, L. H. (1979). *Acta Cryst.* A35, 616–621.
 LEHMANN, M. S. & LARSEN, F. K. (1974). *Acta Cryst.* A30, 580–584.
 NORRESTAM, R. (1972). *Acta Chem. Scand.* 26, 3226–3234.
 SLAUGHTER, M. (1969). *Z. Kristallogr.* 129, 307–318.
 TICKLE, I. J. (1975). *Acta Cryst.* B31, 329–331.
 WAL, H. R. VAN DER, DE BOER, J. L. & VOS, A. (1979). *Acta Cryst.* A35, 685–688.
 WATSON, H. C., SHOTTON, D. M., COX, J. M. & MUIRHEAD, H. (1970). *Nature (London)*, 225, 806–811.
 WERNER, S. A. (1972). *Acta Cryst.* A28, 143–151.

Acta Cryst. (1981). A37, 28–35

Electron Microscopy of Oxyborates.

I. Defect Structures in the Minerals Pinakiolite, Ludwigite, Orthopinakiolite and Takéuchiite

BY JAN-OLOV BOVIN,* M. O'KEEFFE AND M. A. O'KEEFE†

Chemistry Department and Center for Solid State Science, Arizona State University, Tempe, Arizona 85281, USA

(Received 19 October 1979; accepted 13 June 1980)

Abstract

Crystals of the minerals pinakiolite $(\text{Mg}, \text{Mn})_{1.77}(\text{Mn}, \text{Al}, \text{Fe})_{1.11}\text{BO}_5$, ludwigite $(\text{Mg}, \text{Fe})_2\text{Fe}^{3+}\text{BO}_5$, orthopinakiolite $(\text{Mg}, \text{Mn})_{1.85}(\text{Mn}^{3+}, \text{Fe}^{3+})\text{BO}_5$ and takéuchiite $(\text{Mg}, \text{Mn})_{1.97}\text{Mn}_{0.78}^{3+}\text{Fe}_{0.19}^{3+}\text{BO}_5$ have been investigated by high-resolution transmission electron microscopy. Calculated and experimental images have been matched to ensure a proper interpretation. All the minerals except ludwigite show structural defects which give insight into structural relations in the pinakiolite family. It is shown that they can be described as chemical twinings of pinakiolite. The most common defects can be described as missing twin operations.

Takéuchi, Watanabé & Ito (1950) and refined by Moore & Araki (1974). The ludwigite structure was first determined by Takéuchi *et al.* (1950) and several synthetic ferromagnetic compounds with the same structure were reported by Bertaut (1950). The structure of orthopinakiolite was solved by Takéuchi, Haga, Kato & Miura (1978). The present investigation of oxyborates also revealed a new member of the pinakiolite family: takéuchiite (Bovine & O'Keeffe, 1980). Its structure has not yet been determined by X-ray methods but has been deduced from a suggested model (Takéuchi, 1978) by comparing high-resolution

Introduction

This investigation of oxyborates includes the minerals pinakiolite, ludwigite, orthopinakiolite and takéuchiite all with the general formula $M_3\text{BO}_5$, where M stands for different combinations of mainly the ions Mg^{2+} , Mn^{2+} , Fe^{2+} , Mn^{3+} and Fe^{3+} . The crystal structures of pinakiolite, ludwigite and orthopinakiolite have been determined and refined by several groups in the past. Thus the structure of pinakiolite was determined by

Table 1. Chemical formula for $M_3\text{BO}_5$ minerals related to pinakiolite

Mineral & reference	Structural formula
Pinakiolite Moore & Araki (1974)	$\text{Mg}_{1.68}\text{Mn}_{0.09}^{2+}\text{Mn}^{3+}(\text{Al}^{3+}, \text{Fe}^{3+}, \text{Mn}^{4+})_{0.11}\text{BO}_5$
Hulsite Konnert <i>et al.</i> (1976)	$\text{Mg}_{0.64}\text{Fe}_{1.46}^{2+}\text{Fe}_{0.67}^{3+}\text{Sn}_{0.20}^{4+}\text{BO}_5$
Ludwigite Takéuchi <i>et al.</i> (1950)	$(\text{Mg}, \text{Fe}^{2+})_2\text{Fe}^{3+}\text{BO}_5$
Vonsenite Takéuchi (1956)	$\text{Mg}_{0.75}\text{Fe}_{1.25}^{2+}\text{Fe}^{3+}\text{BO}_5$
Orthopinakiolite Takéuchi <i>et al.</i> (1978)	$\text{Mg}_{1.42}\text{Mn}_{0.43}^{2+}\text{Mn}_{0.88}^{3+}\text{Fe}_{0.22}^{3+}\text{BO}_5$
Takéuchiite Bovine & O'Keeffe (1980, 1981)	$\text{Mg}_{1.59}\text{Mn}_{0.42}^{2+}\text{Mn}_{0.78}^{3+}\text{Fe}_{0.19}^{3+}\text{Ti}_{0.01}^{4+}\text{BO}_5$

* Permanent address: Inorganic Chemistry 2, Chemical Centre, PO Box 740, S-220 07, Lund 7, Sweden.

† Present address: University of Cambridge, Department of Physics, Old Cavendish Laboratory, Cambridge CB2 3RQ, England.